NRIAG JOURNAL OF ASTRONOMY AND GEOPHYSICS
2020, VOL. 9, NO. 1, 206–219
https://doi.org/10.1080/20909977.2020.1734998

Hydrogeologic investigations to determine the sources of groundwater recharge of Samalut carbonate aquifer in some wadis, East El Minia, Egypt

Mahmoud A El Ammawy[a], Abdel Galil A Hewaidy[b], Bothaina M Moussa[a], Nabil A Abdel Hafz[b], El Sayed A El Abd[a] and Usama A Abu Risha[a]

[a]Geology Department, Desert Research Center, Cairo, Egypt; [b]Geology Department, Faculty of Science, Al Azhar University, Cairo, Egypt

ABSTRACT
Thirty groundwater samples were collected from wells tapping Samalut fractured carbonate aquifer in the Eastern Desert fringes of the Nile Valley in Minia. The results show a wide variation of groundwater salinity and the graphical presentation of major ion concentrations reflecting variable sources and complex mixing. The inverse evolution modelling shows that the dedolomitization, dissolution of calcite, ion exchange, pyrite and gypsum dissolution are the main mineral–solution interactions controlling the groundwater chemical evolution along flow paths. This study provides evidence on the occurrence of recharge of Samalut aquifer from both the Nile and local floods.

ARTICLE HISTORY
Received 4 November 2019
Revised 2 February 2020
Accepted 11 February 2020

KEYWORDS
Groundwater; recharge; Netpath; desert fringes

1. Introduction

Egypt lies in east Sahara which is the driest part on the planet. Life in Egypt depends mainly on Nile water running from the Ethiopian and central African plateaus. Egypt suffers from extreme water shortage. Looking for groundwater resources and managing them wisely may limit the crisis to some extent. It is important to determine the sources and amounts of groundwater recharge as well as the groundwater storage in the aquifer.

The studied area is bounded by long. 30°43′15”E and 31°30′E and Lat. 27°42′7”N and 28°41′30”N (Figure 1). This area is a part of the western rims of Al-Ma’aza Plateau being bounded from the west by the Nile floodplain. It is a part of the Eastern Desert fringes of the Nile Valley. The area is arid with mean annual rainfall of 22 mm^3/year (Shahin 1985). However, flash floods occur occasionally. For example, a flash flood of 18.5 mm^3/day intensity occurred in November 1994 (EGSMA 1994 and Ashmawy 2002). This flood caused damage of many houses and roads, denudation of wide areas of cultivated lands, and death of thousands of livestock heads.

Under the prevailing aridity, groundwater recharge may occur only from events of similar intensities.

Geomorphologically, the area is divided into limestone plateau, the structural ridges, drainage basins and Recent Nile Alluvial plane (Figure 2).

Geologically, the studied area is covered by sedimentary succession ranging in age from Eocene to Recent (Figure 3). Most of the area is covered by fractured soluble carbonate rocks. As a result of the dissolution of these rocks by floods, karst features were developed. Some of these features formed deep shafts filled with Quaternary sands and gravels (Mostafa 2013). Wide dissolution corridors developed into trunks of several wadis pouring into the Nile (Figure 4). The regional linear structural elements,

the main wadis, and the stratigraphic contacts follow NW-SE trend inhetered from the tectonics formed the Red Sea and Gulf of Suez (Figures 3 and 4).

Groundwater aquifers exist in Samalut and Maghagha formations. Maghagha groundwater has relatively high salinity while the Samalut aquifer groundwater is less saline (El Abd 2015). Based on groundwater levels and salinity distribution, many previous studies show that Samalut aquifer is recharged from the local rainfall, the Nile Irrigation System and the percolation of excess irrigation water (e.g. El Abd et al. 2015). However, the stable isotopes show that the recharge of the Samalut aquifer from the Nile occurred only in the flood season before the construction of the High Dam and ceased after it (Figure 1).

2. Methodology

This study applies multiple GIS, geologic, and hydrogeologic techniques to decipher the hydrogeologic processes that may affect the recharge of Samalut aquifer in east Minia desert fringes. A Garmin global positioning system (GPS) model eTrex 10 was used to define the locations of the collected lithologic and water samples. Lithologic samples from outcrops of Samalut Formation outcrops were collected to compensate for the lack of drilling samples. The collected

CONTACT Mahmoud A El Ammawy elammawymahmoud@yahoo.com Geology Department, Desert Research Center, Cairo, Egypt

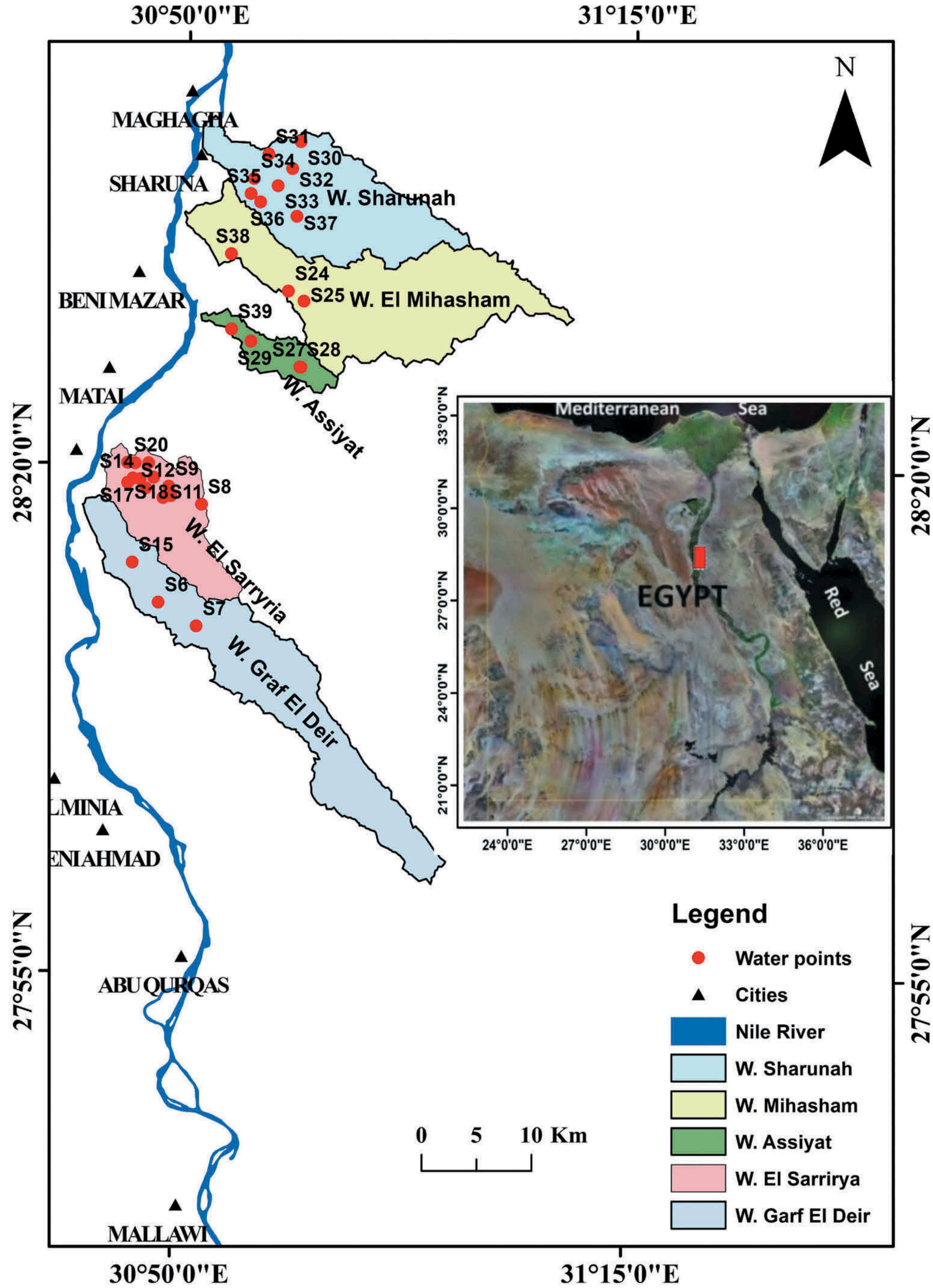

Figure 1. Location of the studied area showing the boundaries of the hydrographic basins.

rock samples were analysed for their lithofacies, mineralogical, and geochemical compositions. Their mineralogical composition was determined using the XRD and their chemical composition was determined by the XRF. Groundwater samples were collected from wells tapping Samalut aquifer in September 2017. Measurements of the pH, and EC of the water samples were taken in the field using calibrated portable metres. Bicarbonate concentrations were determined by titration against sulphuric acid. The concentrations of Ca^{+2}, Mg^{+2}, Na^{+}, K^{+}, SO^{-2}, Cl^{-}, PO_4^{-3} and NO_3^{-} were estimated using a Thermo Scientific Ion Chromatograph (IC), model Dionex, ICS-1100. These analyses were conducted at Laboratories of the Desert Research Centre (DRC) in Cairo, Egypt, according to the methods adopted by the US. Geological Survey (ASTM 2002). The ionic charge balance of these analyses was within ±5%. The concentrations of trace elements were measured using the Induction Coupled Plasma (ICP) at the Desert Research Centre Central Labs.

3. Hydrogeologic setting

The studied Samalut fractured limestone has the characteristics of water-bearing rocks. This is the main

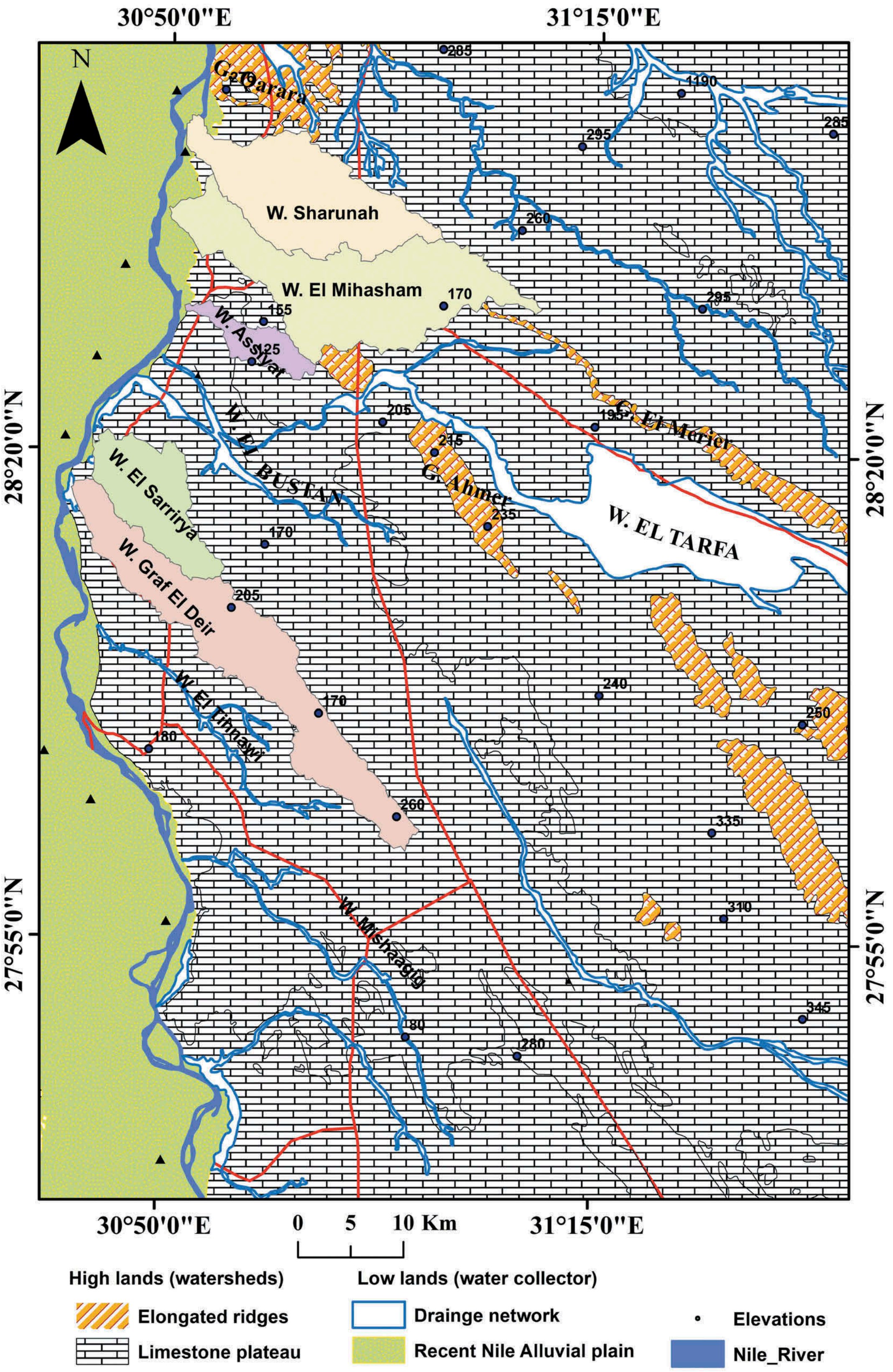

Figure 2. The main geomorphologic units in the studied area.

aquifer with hydrogeologic and hydrochemical characteristics related to the effective conditions and their nature. This aquifer is mainly composed of chalky limestone rich in *Nummulites gizahensis* (Middle Eocene epoch) with effective porosity about 34% (Abdel Tawab 1994) which has given chance to the formation of an aquifer with high potentiality Figure 5.

The groundwater of this aquifer exists under unconfined conditions where the depth to groundwater ranges from 10 m to 08 m. It is represented by 30 water points. It contains fresh groundwater in the southern wadis, but in

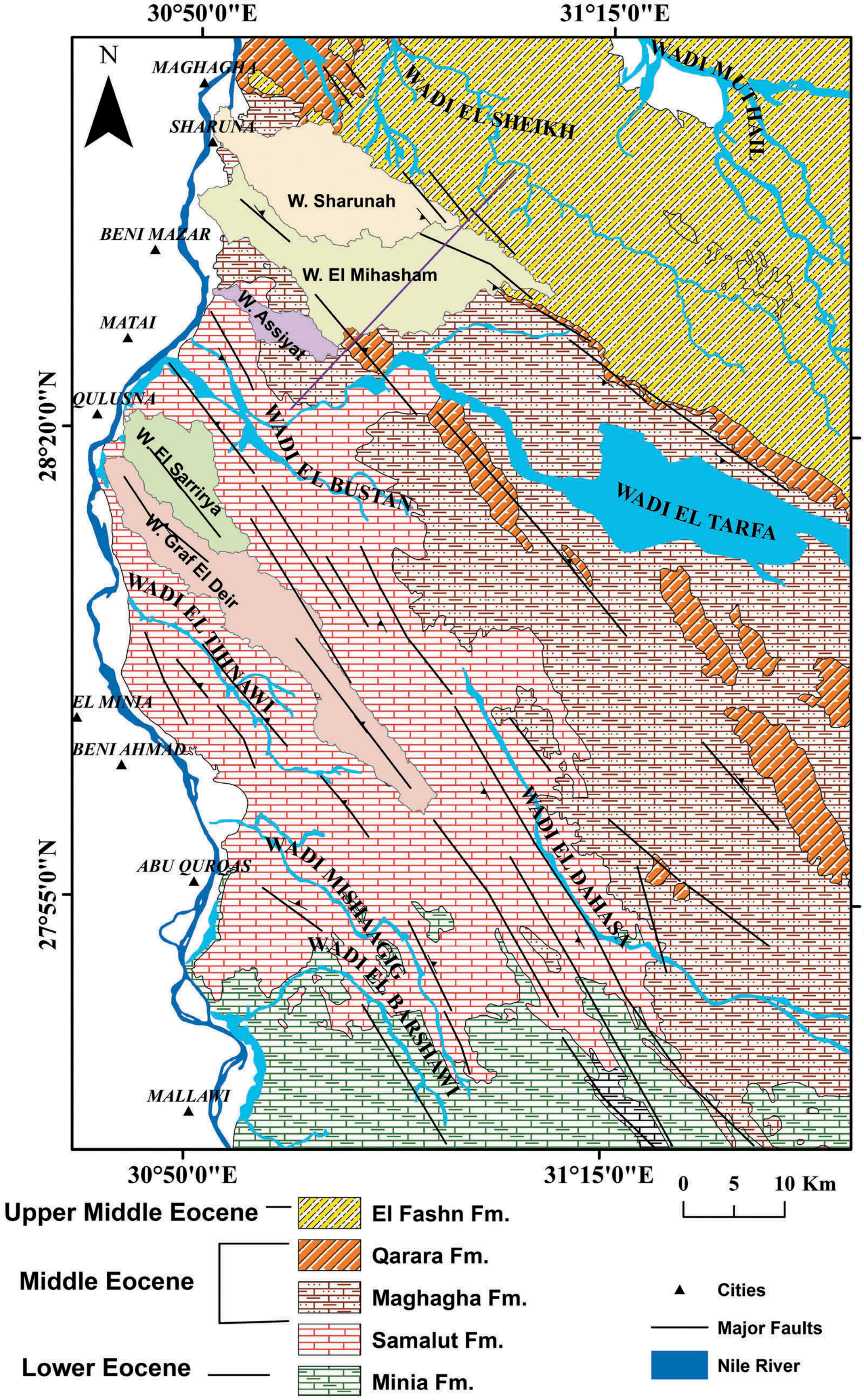

Figure 3. Geology of the area of study (CONOCO 1987).

the northern wadis covered by clays and marls that belong to Maghagha Formation. In this part, it contains more saline water. The aquifer is expected to be connected with the underlying Minia aquifer. In many cases, faulting juxtaposes the Samalut aquifer against the Maghagha aquifer leading to the lateral groundwater flow from one aquifer to the other (Figures 6 and 7) (El Abd 2015).

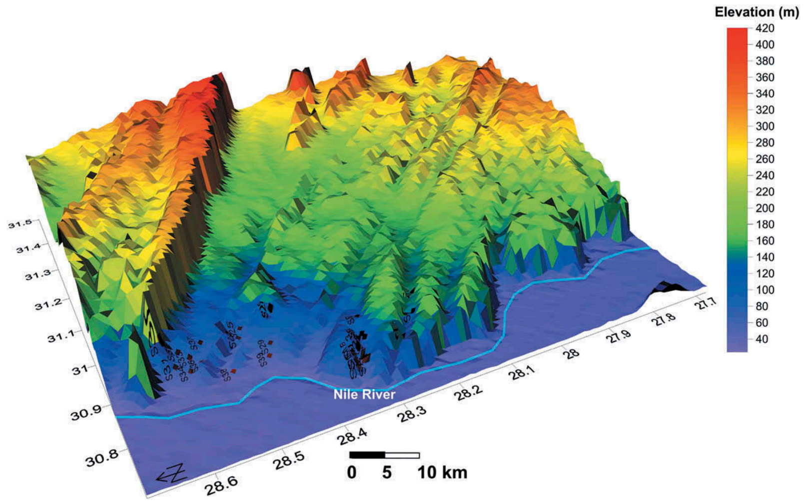

Figure 4. 3-D surface model showing the developed dissolution corridors occupied by the main wadi channels of the Nile drainage system.

Figure 5. Field photographs showing the high discharge of well S18.

4. Results

4.1. Mineralogical associations

The mineralogical composition of the studied rock samples of Samalut Formation is given in Figure 8. Calcite dominates the mineralogical composition followed by the stevensite and anhydrite. CaO dominates the rock chemical composition. The dissolution of calcite is expected to control the groundwater chemistry.

4.2. Depth to water and groundwater temperature

In all studied wadis, there is no specific relationship between groundwater depth and temperature. The temperature of most samples ranges from 26°C to 30°C (Figure 9 and Table 1). This reflects complex mixing of groundwater from different zones in the aquifer. This usually occurs in open holes such as the studied wells. Only sample S20 has a high temperature reflecting possible contribution from deep groundwater zones.

4.3. Water table conditions

The direct relationship between topography (expressed as ground elevation) and depth to water reflects free water table conditions and aquifer hydraulic connection in all the studied wadis. Only three samples deviate from this relationship (Figure 10). They occur in low areas where the groundwater table is deep. This may be due to over pumping.

4.4. Impact of groundwater temperature on its salinity

In general, the groundwater salinity decreases with increasing temperature. This usually occurs in waters with high content of dissolved carbonates, which tends to precipitate with increasing temperature (Appelo and Postma 2005). This agrees with the nature of the aquifer composition. Samples S20 and S27 deviate from this relationship reflecting possible contribution from clastic aquifer zones which are expected to be deep in case of sample S20 and shallower in case of sample S27 (Figure 11).

4.5. Groundwater flow direction and relation to the Nile

The groundwater is available from 30 drilled wells. The depth to water ranges from 15 (S38) m to 109 m (S7). The groundwater level ranges from −15 m.a.s.l. (S17) to 37 m.a.s.l. (S7). The regional groundwater flow is from the southeast to the northwest parallel to the main geologic structures (Figure 12). The level of the water

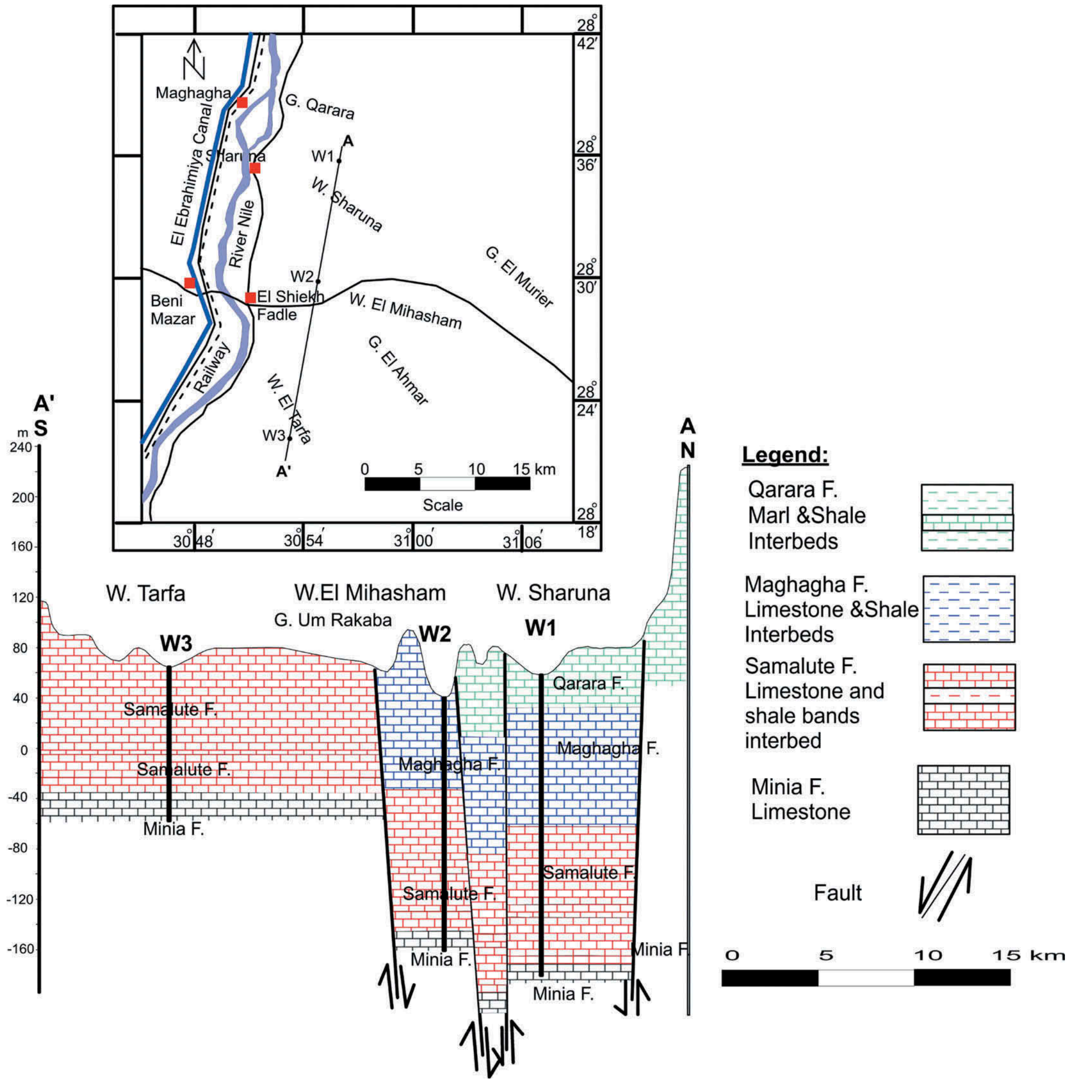

Figure 6. A-A′ NNE-SSW geologic cross-section (El Abd 2015).

in the Nile at Minia ranges from 35 to 36 m.a.s.l. It rises southward of Minia and declines to the north.

4.6. Groundwater salinity distribution

The groundwater salinity in Samalut aquifer varies from 350 ppm (S13) to 2043 ppm (S27) (Figure 13). Generally, the salinity increases in the same direction of groundwater flow. The high salinity of some groundwater points can be attributed to the dissolution of carbonate rocks, the connection with Maghagha aquifer, and the high contribution of recharge from seasonal floods. The areas with low salinity are expected to contain groundwater recharged predominantly from the Nile flooding before the construction of the High Dam.

4.7. Water level–Salinity relationship

Generally, there is no specific relationship between groundwater levels and its salinity (Figure 14). However, some samples in Wadi Al-Sarrirya show increasing salinity with increasing water level which may reflect mixing with groundwater from the overlying Maghagha aquifer. Only sample S20 is expected to represent aquifer zone connected with deeper semi-confined clastic zones.

4.8. Major ion recharge indicators

The wide range of major ion concentrations (Table 2) and the occurrence of different groundwater types and dissolved salts (Table 3) reflect complicated recharge, mixing and water–rock interactions. The percent of the groundwater dissolved bicarbonates increases towards the wadis Al Muhasham, Al Assyiat, and Garf El Deir (Figure 15) reflecting recharge from the river. No bicarbonate trend exists in Wadi Sharuna. However, in Wadi El Sarrirya and Wadi Garf El Deir, the wells exist in the middle of these wadis have higher bicarbonate percentages compared to the wells in their sides. These wells may receive recharge through preferred paths along open fractures or fault plains. The

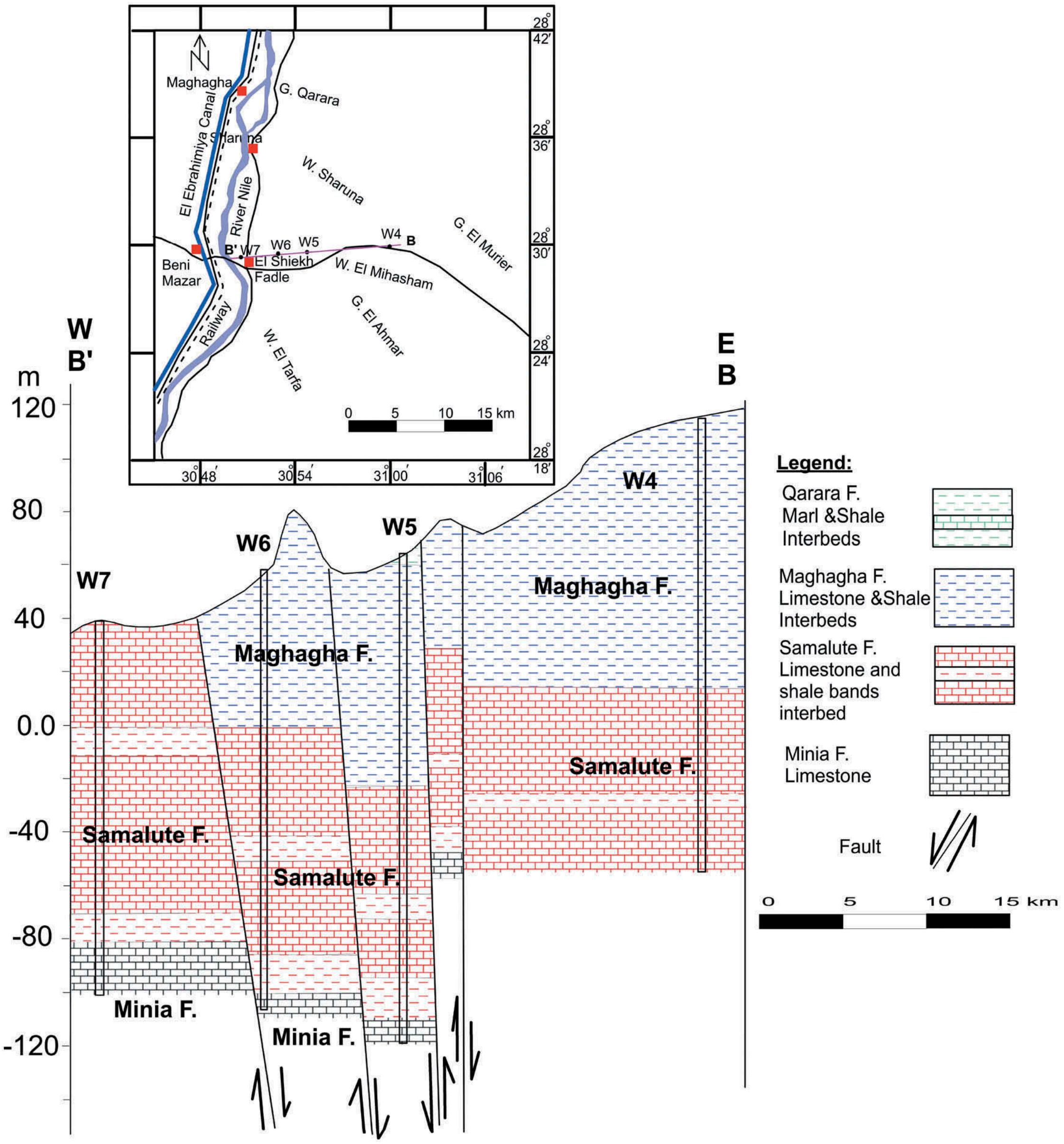

Figure 7. B-B′ E-W geologic cross-section (El Abd 2015).

magnesium concentrations are high as well as the magnesium bicarbonate (Tables 3 and 4), with clear decrease of calcium concentration and calcium bicarbonate in all samples except sample S6 and S7.interactionwith non-marine strata, which may

This reflects dedolomitization process associated with calcite precipitation as can be concluded from the low Ca/Mg ratios (Table 3). Gypsum is also expected to dissolve resulting in high sulphate concentrations in most groundwater samples (Table 2). The decrease of bicarbonate concentrations with increasing salinity (Figure 16) is a continuous process controlled by natural logarithmic relationship. From the aforementioned data, recharge from flash floods and subsequent mixing with the water recharged from the Nile is also expected. The rNa/rCl ≈1 reflecting the dissolution of halite. The fact that the examined rock samples lack halite in their composition reflects that the halite dissolution occurred in the past with complete leaching of this mineral from the rock matrix. So, for young groundwater, Cl behaves conservatively along the flowpaths before start mixing with the older groundwater in the deeper parts of the aquifer. The occurrence of the Na_2SO_4 salt reflects the interaction with non-marine strata, which may occur during the recharge.

4.9. *Inverse hydrogeochemical modelling*

The aim of this modelling approach is to test the possibility of recharge from both the Nile and flash floods with subsequent mixing between the accumulated groundwater plumes. Three modelling steps have been done using Netpath (Plummer et al. 1994) to accomplish this goal as follows:

4.9.1. *Recharge from the Nile*

In this step, sample S13 is assumed to be recharge completely from the Nile based on its low salinity

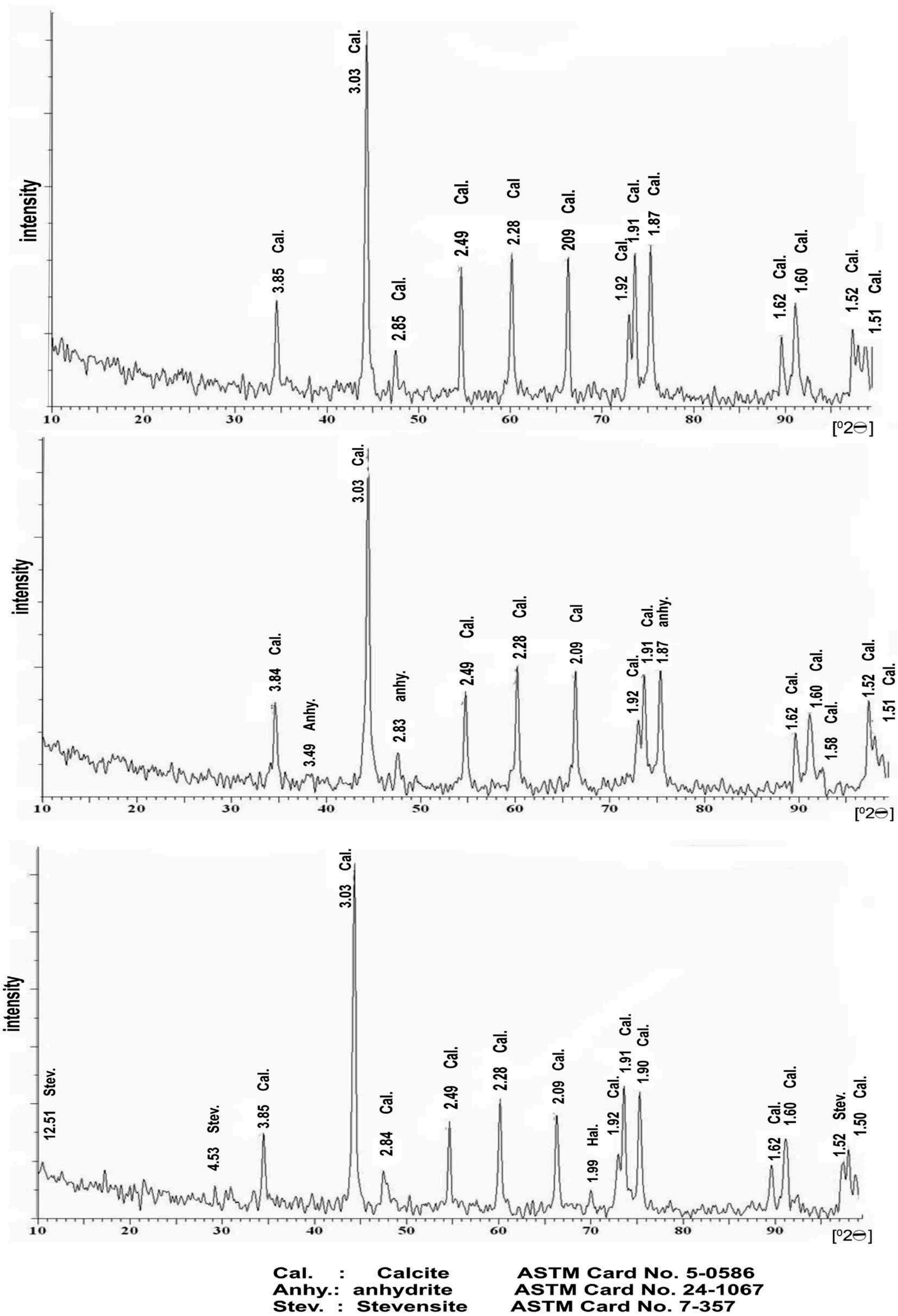

Figure 8. X-ray data of bulk samples in Samalut formation.

and high bicarbonate (Figure 16). The dedolomitization and gypsum and removal of calcium via calcite precipitation and inverse ion exchange for sodium are the main interactive processes (Table 5). According to Figure 8 no gypsum was found in the aquifer rocks. In this case, pyrite dissolution takes place.

4.9.2. Recharge from flash floods

In this step, sample S28 is assumed to be recharged from the flash floods affected by evaporation. The main interactions are calcite and pyrite precipitation, dolomite and gypsum dissolution, and inverse ion exchange (Table 5). The reason for evaporation incorporation in the model is the arid nature of the region.

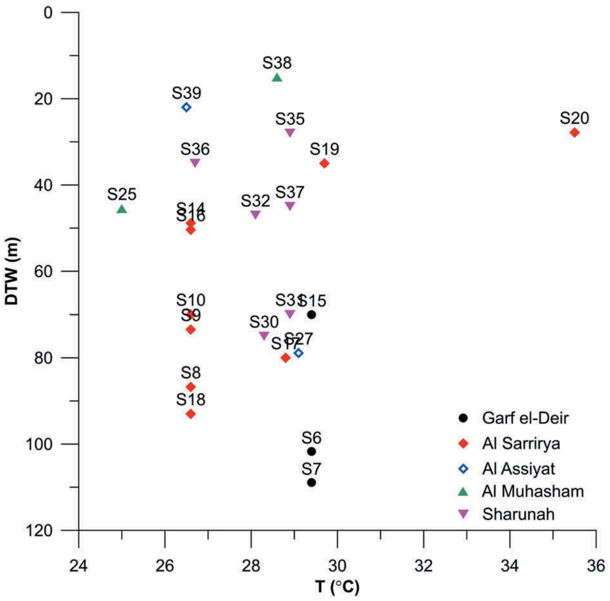

Figure 9. The relationship between groundwater temperature and its depth.

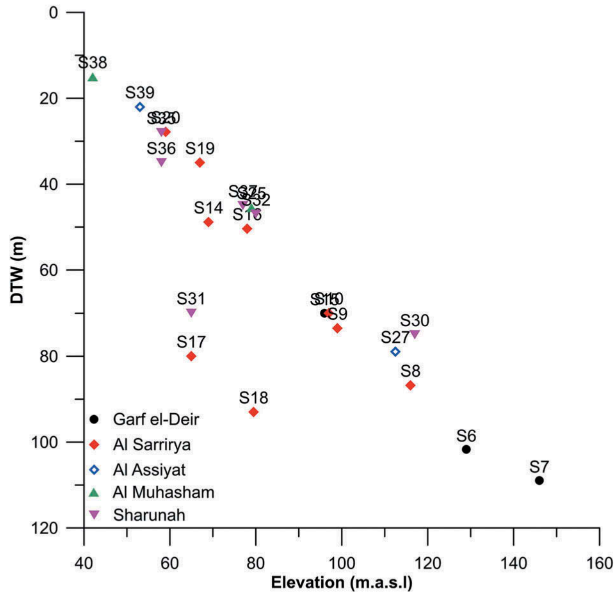

Figure 10. Relationship between topography and depth to water.

The impact of evaporation on the recharge water cannot be ignored.

4.9.3. Mixing

In this step, the sample S24 occurring in the middle of Wadi Al-Muhasham is assumed to be the result of mixing between the upstream sample (S25) which is assumed to be recharge from flash floods and the downstream sample (S38) which is assumed to be recharged from the Nile. The dissolution of dedolomitization and precipitation of calcite and pyrite in addition to the exchange of Mg in the rocks for Na in solution are the main water–rock interactions controlling the evolution of the final sample S24 (Table 5).

5. Discussion

5.1. Sources of recharge

The Eastern Desert of Egypt contains multiple aquifers. The majority of these aquifers are relatively poor

Table 1. Field measurements and salinity of the collected groundwater samples.

No.	TD (m)	DTW (m)	Elev (m.a.s.l.)	WL (m.a.s.l.)	T (ºC)	EC (µS/cm)	PH	TDS (mg/l)	Wadi
S6	29.4	101.7	129	27.3		710	8.1	424.5	Garf El-Deir
S7	29.4	108.92	146	37.08		900	8	561.1	Garf El-Deir
S15	130	70	96	26	29.4	1050	8	669.6	Garf El-Deir
S8	26.6	86.77	116	29.23		1106	8	719.6	El Sarrirya
S9	26.6	73.47	99	25.53		600	7.7	399.5	El Sarrirya
S10	100	70	97	27	26.6	600	7.8	422.2	El Sarrirya
S11						680		448	El Sarrirya
S12						2200		1264.1	El Sarrirya
S13					30.4	640	8	349.7	El Sarrirya
S14	134	48.83	69	20.17	26.6	2890	7.7	1523.2	El Sarrirya
S16	94	50.38	78	27.62	26.6	1640	8.1	932.7	El Sarrirya
S17	44.31	80	65	−15	28.8	630	8	422.8	El Sarrirya
S18	50	93	79.5	−13.5	26.6	1350	8	782.4	El Sarrirya
S19	90	35	67	32	29.7	930	8	559.3	El Sarrirya
S20	100	27.81	59	31.19	35.5	3250	8	2027.9	El Sarrirya
S27	145	78.92	112.5	33.58	29.1	3550	8.3	2043.9	El Assiyat
S28	175				26.9	2180	8.6	1278.1	El Assiyat
S29					26.9	1460	8.8	762.4	El Assiyat
S39	105	22	53	31	26.5	1060	8.8	657.2	El Assiyat
S24	216					1520	8.8	862.5	El Muhasham
S25	180	45.47	79	33.53	25	1780	8.4	978.5	El Muhasham
S38	110	15	42	27	28.6	980	8.9	603.5	El Muhasham
S30	253	75	117	42	28.3	1660	8.8	873.1	Sharunah
S31	250	70	65	−5	28.9	1600	8.7	880	Sharunah
S32	260	47	80	33	28.1	1580	8.7	881.1	Sharunah
S33						1980		1090.5	Sharunah
S34					29.7	1680	8.7	887.1	Sharunah
S35	200	28	58	30	28.9	1590	8.7	884.7	Sharunah
S36	170	35	58	23	26.7	1600	8.9	888.7	Sharunah
S37	220	45	77	32	28.9	1820	8.7	976.8	Sharunah

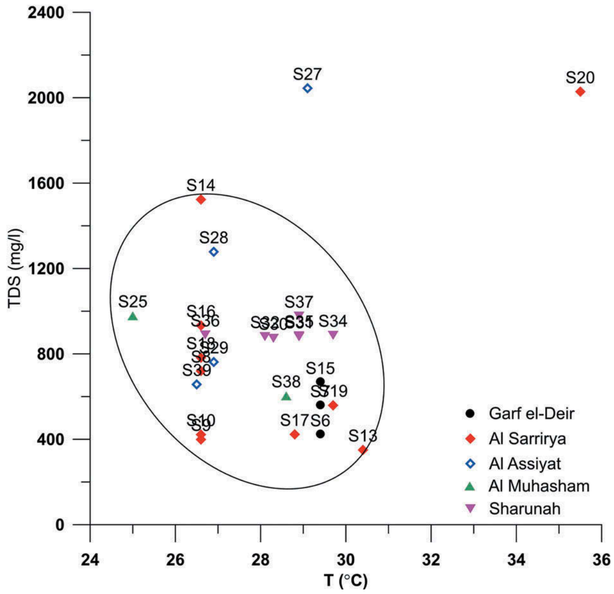

Figure 11. Effect of groundwater temperature on its salinity.

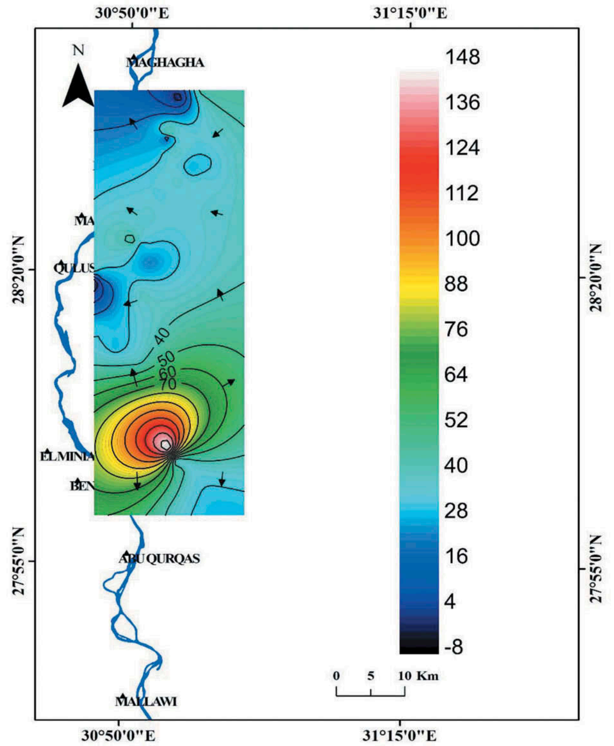

Figure 12. Water table map of the Samalut aquifer (September 2017); the local low anomalies are predominantly due to overpumping.

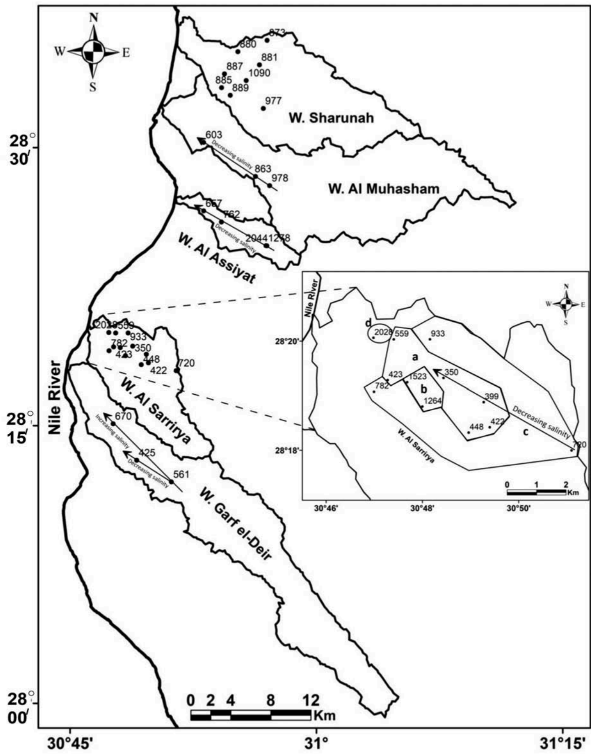

Figure 13. Groundwater salinity distribution (for well numbers refer to Figure 1).

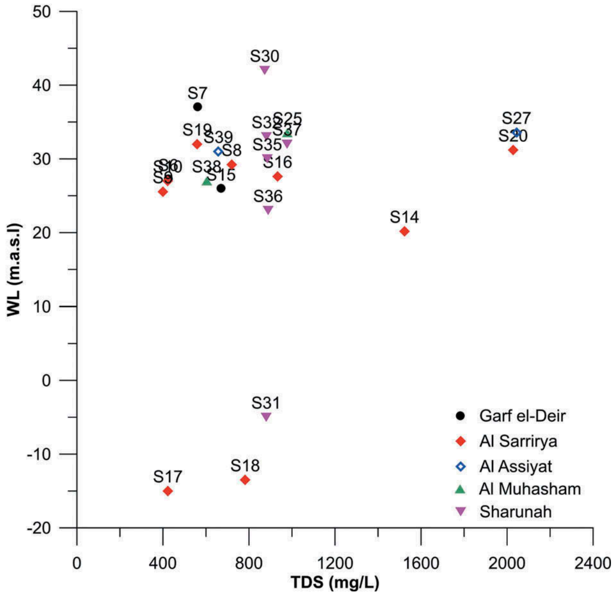

Figure 14. Salinity–water level relationship.

in groundwater storage as they recharge completely from seasonal floods. Contrarily, the carbonate aquifers of the Nile desert fringes are of good potentiality. As all these aquifers exist in the same climatic region, the desert fringes' aquifers are expected to receive recharge from sources other than the flash floods. Many studies show that these aquifers receive recharge from the Nile.

The relationship between the Nile and the aquifers bounding its course and valley is one of the major controversies among scientists. However, most of the previous studies addressed this issue based on the water level measurements. (El Kashouty 2010) attributed the recharge of the Eocene carbonate aquifer between Minia and Beni Suef to lateral flow from the surrounding aquifers and the return of the excess irrigation water. Tamer and Rachwan (1987), Awad et al. (1997) and Korany et al. (2013) attributed the recharge of this aquifer at Assiut to the flash floods and the upward leakage of groundwater from the Nubian Sandstone aquifer. At west Abu Qurqas (Al Temamy

Table 2. Major ion concentrations in groundwater samples.

No.	Ca mg/l	Mg mg/l	Na mg/l	K mg/l	CO_3 mg/l	HCO_3 mg/l	SO_4 mg/l	Cl mg/l
S6	27.5	68.8	37.5	6.4	24	414.8	14.0	39.0
S7	31.6	65.8	85.6	6.7	30	378.2	44.1	108.2
S15	34.9	79.4	90.7	6.9	24	353.8	128.6	128.2
S8	37.9	93.2	103.1	5.5	12	353.8	63.3	227.7
S9	26.3	65.1	34.7	5.5	22	412.2	10.6	29.2
S10	26.7	68.3	38.4	5.1	24	408.7	14.8	40.5
S11	28.8	69.4	43.5	5.5	36	375.8	12.4	64.6
S12	63.3	144.8	210.7	9.7	18	427.0	138.8	465.3
S13	26.1	53.0	37.2	6.4	18	366.0	14.9	11.1
S14	65.2	160.5	275.1	10.2	6	329.4	196.7	644.8
S16	28.0	104.3	139.4	9.7	6	311.1	345.7	144.0
S17	27.3	73.1	36.1	5.8	18	427.0	15.1	33.9
S18	35.5	101.2	114.2	5.7	2	385.5	170.4	160.2
S19	32.9	81.1	64.3	4.2	12	390.4	96.0	73.6
S20	39.9	161.2	432.7	16.4	18	419.2	553.1	597.0
S27	43.9	162.9	446.9	22.4	6	390.4	404.4	762.2
S28	60.1	142.2	211.6	9.9	18	390.4	232.4	408.7
S29	35.9	105.5	114.4	5.5	36	372.1	67.4	211.6
S39	35.1	64.8	120.6	6.3	30	405.3	64.8	132.9
S24	29.0	105.0	138.7	11.7	18	400.9	105.1	254.6
S25	31.9	112.6	147.8	13.1	24	373.2	134.9	327.6
S38	36.0	92.6	61.4	4.8	48	382.6	54.1	115.1
S30	29.0	105.2	138.2	10.9	6	390.4	117.5	271.1
S31	28.4	104.2	137.4	11.8	24	359.9	112.9	281.5
S32	29.4	108.2	139.4	11.1	24	348.2	112.1	282.8
S33	49.8	115.2	185.3	10.7	18	407.0	112.3	395.7
S34	30.2	107.3	141.2	10.1	12	390.4	113.1	277.9
S35	28.7	108.3	139.9	12.0	36	313.8	117.7	285.3
S36	29.8	110.5	142.7	10.0	12	396.0	114.6	271.0
S37	34.1	118.3	150.8	11.5	12	390.4	142.8	312.1
Nilea	31	6.58	37.5	4.5		189	8	13.31
Raina	12.2	2.5	49	5.7		121	19	26.7

Al Temamy and Abu Risha (2016).

Table 3. Hydrochemical coefficients of the studied groundwater samples.

Well no.	rNa/rCl	rSO4/rCl	rCa/rMg	(Ca+Mg)/Cl	Ca/Na	Mg/Na	(Ca+Mg)/Na	Ca/Mg
S6	1.7	0.3	0.2	3.2	0.4	1.7	2.2	0.2
S7	1.3	0.3	0.3	1.1	0.2	0.7	0.9	0.3
S15	1.2	0.7	0.3	1.1	0.2	0.8	1.0	0.3
S8	0.7	0.2	0.2	0.7	0.2	0.9	1.1	0.2
S9	2.1	0.3	0.2	4.0	0.4	1.8	2.2	0.2
S10	1.6	0.3	0.2	3.0	0.4	1.7	2.1	0.2
S11	1.1	0.1	0.3	2.0	0.4	1.5	1.9	0.3
S12	0.7	0.2	0.3	0.6	0.2	0.7	0.8	0.3
S13	5.5	1.0	0.3	9.1	0.4	1.3	1.8	0.3
S14	0.7	0.2	0.2	0.5	0.1	0.6	0.7	0.2
S16	1.6	1.8	0.2	1.2	0.1	0.7	0.8	0.2
S17	1.8	0.3	0.2	3.9	0.4	1.9	2.3	0.2
S18	1.1	0.8	0.2	1.1	0.2	0.8	1.0	0.2
S19	1.4	1.0	0.2	2.0	0.3	1.2	1.5	0.2
S20	1.2	0.7	0.2	0.5	0.1	0.4	0.4	0.2
S27	1.0	0.4	0.2	0.4	0.1	0.3	0.4	0.2
S28	0.8	0.4	0.3	0.6	0.2	0.6	0.8	0.3
S29	0.8	0.2	0.2	0.9	0.2	0.9	1.1	0.2
S39	1.5	0.4	0.3	0.9	0.2	0.5	0.7	0.3
S24	0.9	0.3	0.2	0.7	0.1	0.7	0.8	0.2
S25	0.8	0.3	0.2	0.6	0.1	0.7	0.8	0.2
S38	0.9	0.3	0.2	1.5	0.3	1.4	1.8	0.2
S30	0.8	0.3	0.2	0.7	0.1	0.7	0.8	0.2
S31	0.8	0.3	0.2	0.6	0.1	0.7	0.8	0.2
S32	0.8	0.3	0.2	0.6	0.1	0.7	0.9	0.2
S33	0.8	0.2	0.3	0.5	0.2	0.6	0.7	0.3
S34	0.8	0.3	0.2	0.7	0.1	0.7	0.8	0.2
S35	0.8	0.3	0.2	0.6	0.1	0.7	0.8	0.2
S36	0.8	0.3	0.2	0.7	0.1	0.7	0.9	0.2
S37	0.8	0.3	0.2	0.6	0.1	0.7	0.9	0.2

and Abu Risha 2016) attributed recharge of the Eocene aquifer to all aforementioned sources.

The plots of groundwater isotopes lie along a mixing line below the global meteoric water line (Craig 1961) (Table 6, Figure 17). Some samples plot on Alexandria local meteoric water line (IAEA/WMO 1998). The groundwater levels in the vicinity of the Nile are lower than that of the Nile water implying the occurrence of recharge from the Nile. However, some studies state that the recharge from

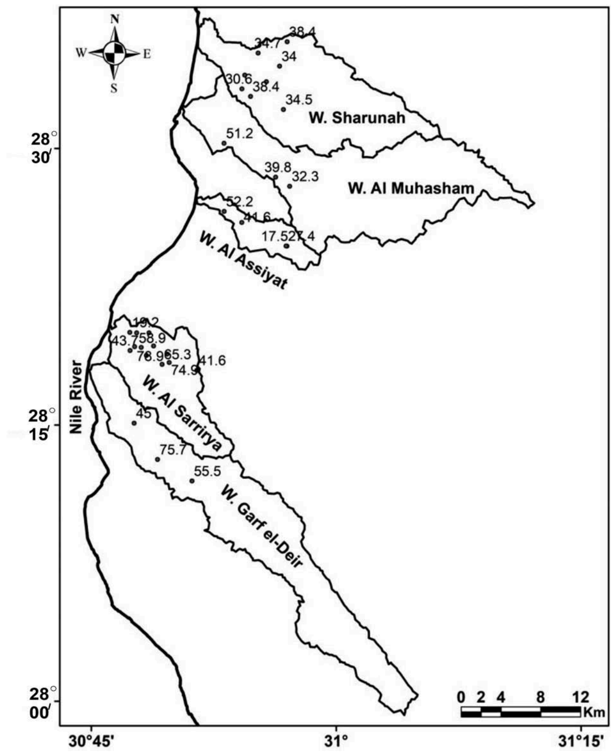

Figure 15. HCO_3% reflects recharge from the Nile. For well numbers refer to Figure 1.

Table 4. Hypothetical salts of the studied groundwater samples.

Well no.	NaCl	Na_2SO_4	$NaHCO_3$	$MgCl_2$	$MgSO_4$	$Mg(HCO_3)_2$	$Ca(HCO_3)_2$
S6	12.2	3.2	4.9				79.6
S7	27.3	8.2	0.2				64.2
S15	28.0	5.2			15.5	37.2	14.0
S8	32.6			13.4	9.4	31.1	13.4
S9	9.7	2.6	7.6			64.4	15.8
S10	12.8	3.4	4.4			64.2	15.3
S11	19.3	2.7	0.1			62.2	15.7
S12	38.5			17.1	12.2	19.3	12.9
S13	4.3	4.3	15.3			58.6	17.5
S14	42.6			22.6	14.7	8.7	11.3
S16	24.5	14.2			29.2	23.4	8.6
S17	10.8	3.5	4.6			66.1	15.0
S18	31.2	2.4			22.1	32.6	11.6
S19	19.1	6.8			11.5	47.9	14.6
S20	47.0	8.8			23.3	15.1	5.8
S27	56.2			2.7	23.0	11.9	6.2
S28	39.2			10.2	20.7	17.5	12.4
S29	32.8			7.8	9.6	38.3	11.5
S39	29.4	10.6	3.3			42.6	14.0
S24	38.6			4.8	13.2	34.6	8.8
S25	38.4			10.3	14.8	27.4	9.0
S38	22.9			3.6	9.2	49.6	14.7
S30	38.4			7.4	14.6	30.7	8.8
S31	38.6			8.1	13.8	30.8	8.7
S32	38.0			9.4	13.9	29.9	8.8
S33	41.1			12.7	11.2	22.8	12.2
S34	38.3			7.9	13.8	31.0	9.0
S35	38.2			9.5	14.5	29.1	8.6
S36	38.0			7.2	14.1	32.0	8.7
S37	37.5			9.9	16.0	27.3	9.3

the Nile used to occur only before the construction of the High Dam during the Nile flood season and such recharge has ceased after the construction of the dam (e.g. Kebede et al. 2017). The isotopes of groundwater

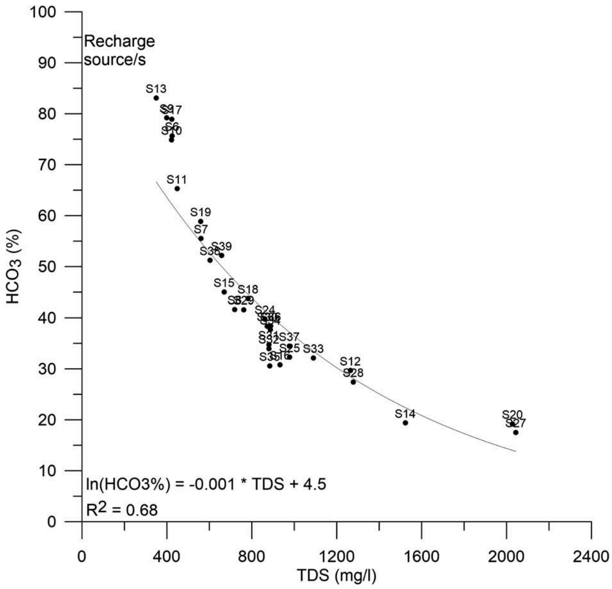

Figure 16. Relationship between groundwater salinity (TDS) and bicarbonate concentration.

in the study area are very different from the current isotopic signature of the Nile water as well as from the long-term average weighted mean (LTAWM) isotope content of rainfall at Alexandria (Figure 17; IAEA/WMO 1998; Ibrahim and Lyons 2017). Accordingly, no current recharge from the Nile is expected. The Nile Valley being composed mainly of silt is expected to act as a barrier between the Nile and the aquifer. The stable isotopes of other group of groundwater samples are relatively similar to that of the Eastern Desert floodwater (Hamza et al. 1999) reflecting the occurrence of recharge from local floods. Sample 33 is expected to be a mixture of group A and group B (Figure 17) groundwater. The stable isotopes support the aforementioned modelling approach.

In Summary, the isotopic measurements show that the groundwater has a signature that is quite different from that of the Nile water and the winter rainwater (Alexandria rainwater isotopes). However, mixing between these end members produce isotopic signature similar to that of some groundwater samples (Figure 17).

Groundwater upwelling from the Nubian aquifer has not been found in the area of study based on the available data. There is no evidence on the percolation of excess irrigation water as the isotopic signature of groundwater is much depleted compared to the isotopic signature of the canal irrigation waters. Contrarily, the depleted istopic signature of canal water relative to the Nile water (Awad et al. 1997; Korany et al. 2013) has been attributed to groundwater discharge from the aquifers into the irrigation drains (El-Bakri et al. 1996) and canals (Hamza et al. 1999). Some samples are sourced from deep clastic zones (e.g. S20).

Table 5. Results of the inverse hydrogeochemical modelling. Negative figures mean removal from solution (i.e. precipitation of solute) and vice versa.

Model		Recharge from Nile		Recharge from floods+ evaporation		Mixing		
waters		Initial Nile water	Final S13	Initial Flood	Final S28	Initial 1 38 66%	Initial 2 25 34%	Final 24
Phases		Cal., Dol., +Gyp., Exch., Pyr.		Cal., Dol., +Gyp., Ex., Pyr.		Cal., Dol., +Gyp., Ex., Pyr., Mg/Na Ex.		
Constraints		Ca, Mg, Na, S		Ca, Mg, Na, S, C, Cl		Ca, S, Cl, Na, Mg		
Reactions (mmol/l)	Cal.	−2.04		−0.704		−0.53		
	Dol.	1.9		0.074		0.42		
	Pyr.	0.036		−0.17		−0.01		
	Gyp^+.			0.039				
	Exch.	−0.006		−0.108				
	Mg/Na Ex					0.45		
	Ev. F			13.2				
	H_2Or			75.75				

Table 6. Stable isotopes of groundwater samples (Korany et al. 2013) and additional reference samples.

Sample No.	Cl	$\delta^{18}O$	^2H	References
25	4.99	−1.45	−9.03	Korany et al. (2013)
26	4.87	−1.72	−8.9	
27	4.88	−2.08	−10.8	
29	19.51	−0.32	2.59	
30	10.09	−0.7	4.87	
31	0.91	−0.55	4.91	
32	5.41	−0.55	5.37	
33	2.77	−1.22	−1.44	
Ethiopian rain		−2.5	−5	Ethiopian rain
Nile before High dam		−0.92	2.55	Hamza et al. (1999)
Nile at Minia (Av.)		3.01	26.9	El-Bakri et al. 1996
Surface water Av.		2.91	24.69	Awad et al. 1997; El-Bakri et al. 1996; Keatings et al. (2007) and Korany et al. (2013)
Alex rain LTAWM		−3.97047	−15.6045	IAEA
ED floods		−1	−5	Hamza et al. (1999)

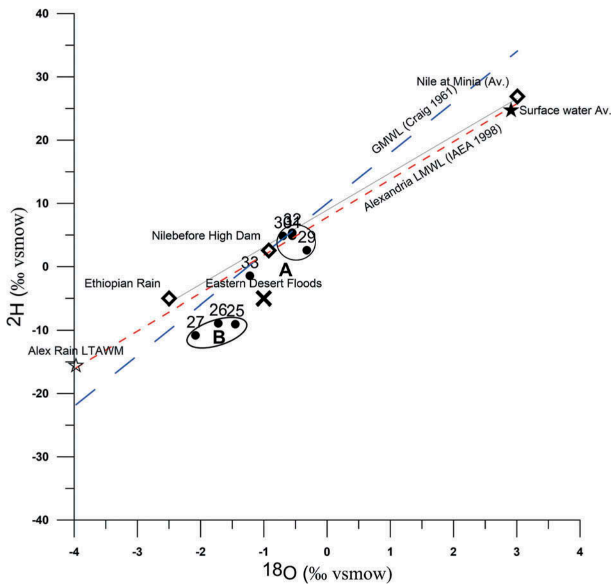

Figure 17. ^{18}O-^{2}H relationship showing the groundwater recharge from the Nile before the construction of the High Dam and from the seasonal.

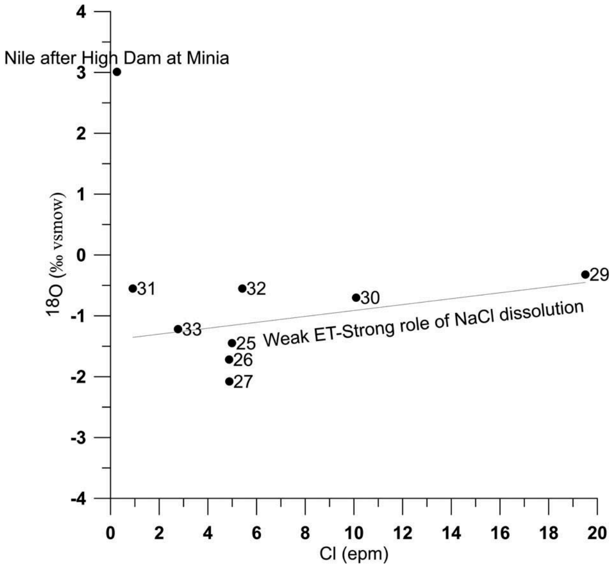

Figure 18. Relationship between Cl and ^{18}O concentration.

5.2. Halite dissolution

The Cl-^{18}O pattern reflects dissolution of halite (Ibrahim and Lyons 2017; Figure 18). This means that Cl does not conservative. As Cl is assumed to be conservative and its concentrations were used to estimate the contributions from the end members to the final sample in the Netpath mixing model, the results of this model must be dealt with due caution.

6. Conclusions

The groundwater Samalut aquifer was recharged mainly from the Nile flooding before the High Dam construction. If the recharge occurs from the current Nile, it must mix with another water of isotopic signature similar to that of the rainwater at Alexandria. The same is applicable to recharge from irrigation-drainage system. Recharge from seasonal flash floods in the Eastern Desert occurs. It forms groundwater with high salinity compared to the groundwater recharged from the Nile. This water gradually mixes with the main fresh groundwater body. No groundwater upwelling from the Nubian aquifer has been defined so far in the study area. This study demonstrates the ability of major ions in defining the sources of recharge. However, the stable isotopes are more accurate in doing this.

Disclosure Statement

No potential conflict of interest was reported by the authors.

References

Abdel Tawab S. 1994. A geotechnical evaluation of Minia-Maghagha area upper Egypt. Earth Sci. 7:143–157.

Al Temamy AM, Abu Risha UA. 2016. Groundwater interaction and potential inferred from geoelectrical and hydrogeological techniques in the desert fringe of Abu Qurqas area, El Minia, West Nile, Egypt. Egypt J Geol. 60:75–95.

American Society for Testing and Materials (ASTM). 2002. Water and environmental technology. Annual book of ASTM standards, USA, Sec. 11, vols 11.01, and11.02. West Conshohocken: ASTM International.

Appelo CAJ, Postma D. 2005. Geochemistry, groundwater and pollution. 2 ed. Leiden (The Netherlands): A.A. Balkema; p. 649.

Ashmawy MH. 2002. Surface runoff potentiality and hazards of drainage basins along the eastern side of the Nile valley between Asyut and Al-Minia, Egypt. Egy J Geol. 46–1:283–300.

Awad MA, El Arabi EN, Hamza MS. 1997. Use of solute chemistry and isotope to identify sources of groundwater recharge in the Nile aquifer system, upper Egypt. Ground Water. 35(2):223–228.

Continental Oil Company (CONOCO). 1987. Geologic map of Egypt. Egyptian general authority for petroleum (UNESCO joint map project), 20 sheets, scale 1:500, 000. Cairo: General Petroleum Company.

Craig H. 1961. Isotopic variations in natural waters. Science. 133:1702–1703.

Egyptian Geological Survey and Mining Authority (EGSMA). 1994. Flash floods of November 1994. Cairo: Upper Egypt Governorates (in Arabic).

El Abd E. 2015. Hydrogeological study of the groundwater aquifers in the reclamation area of the desert fringes east Nile between Biba – el Fashn, Eastern Desert, Egypt. Egyptian J Pure Applied Sci. 53–4:13–25.

El Abd EA, Salem AA, Ghoubachi SY. 2015. Geological impact on the groundwater occurrence in the area East El-sheikh Fadl, El Minia governorate, Egypt. Sedimentology Egypt. 22:169, 183.

El Kashouty M. 2010. Modeling of the limestone aquifer using isotopes, major, and trace elements in the western River Nile between Beni Suef and El Menia. Cairo (Egypt): IWTC14; p. 941–968.

El-Bakri A, Tantawi MA, Hamza MS, Awad MA. 1996. Estimation of groundwater inflow to irrigation drains in Minia, upper Egypt, based on a deuterium and oxygen-18 evaporation pan technique. Hydrol Sci J. 41(1):41–48.

Hamza MS, Aly AIM, Awad MA, Nada AA, Abdel-Samie SG, Sadek MA, Salem WM, Attia FA, Hassan TM, El-Arabi NE, et al.1999. Estimation of recharge from Nile Aquifer to the desert fringes at Qena area, Egypt. Isotope techniques in water resources development and management symposium (1999), inter. atomic energy agency, Vienna; p. 34–46. IAEA-CSP-2/C, session 4.

IAEA/WMO. 1998. Global network of isotopes in precipitation. The GNIP Database. http://www.iaea.org/programs/ri/gnip/gnipmain.htm

Ibrahim RGM, Lyons WB. 2017. Assessment of the hydrogeochemical processes affecting groundwater quality in the Eocene limestone aquifer at the desert fringes of El Minia Governorate, Egypt. Aquat Geochem. 23:33–52.

Keatings K, Tassie GJ, Flower RJ, Hassan FA, Hamdan MAR, Hughes M, Arrowsmith C. 2007. An examination of groundwater within the hawara pyramid, Egypt. Geoarchaeology. 22(5):533e554.

Kebede S, Abdalla O, Sefelnasr A, Tindimugaya C, Mustafa O. 2017. Interaction of surface water and groundwater in the Nile River basin: isotopic and piezometric evidence. Hydrogeol J. 25:707–726.

Korany EA, Tempel RN, Gomaa MA, Mohamed RG. 2013. Detecting the roles of the physiochemical processes on groundwater evolution, Assiut area, Egypt-applications of hydrogeochemical and isotopic approaches. Egypt J Geol. 57:63–83.

Mostafa A. 2013. Paleokarst shafts in the western desert of Egypt: a unique landscape. Acta Carsologica. 42 (1):49–60.

Plummer LN, Prestemon EC, Parkhurst DL. 1994. An interactive code (NETPATH) for modelling NET geochemical reactions along a flow PATH, version 2.0. U.S. Geological survey, water-resources investigations. Report 94/4169.

Shahin MM. 1985. Hydrology of the Nile Basin. Amsterdam: Elseveir; p. 575.

Tamer MA, Rachwan MA. 1987. Hydrogeological studies on the Cenozoic clastic aquifers in the area between Aswan and Assiut. Desert Inst Bull. 37(1):37–52. A. R. E.